Available online at www.sciencedirect.com

ScienceDirect

www.elsevier.com/locate/jes

JES JOURNAL OF ENVIRONMENTAL SCIENCES

www.jesc.ac.cn

Effect of sodium alginate on phosphorus recovery by vivianite precipitation

Cong Zhang, Dexiu Hu, Ruijie Yang, Zichen Liu*

State Key Laboratory of Eco-hydraulics in Northwest Arid Region of China, Xi'an University of Technology, Xi'an 710048, China

ARTICLE INFO

Article history:
Received 4 February 2020
Revised 3 April 2020
Accepted 4 April 2020
Available online 16 April 2020

Keywords:
Phosphorus recovery
Excess sludge
Vivianite
Sodium alginate

ABSTRACT

There are good prospects for phosphorus recovery from excess sludge by vivianite crystallization while a large number of extracellular polymeric substances in sludge will have impact on vivianite precipitation. In this study, as a representative of extracellular polymeric substance, the effect of sodium alginate (SA) on phosphorus recovery by vivianite precipitation under different initial SA concentrations (0–800 mg/L), pH values (6.5–9.0) and Fe/P molar ratios (1:1–2.4:1) was investigated using synthetic wastewater. The results showed that SA in low concentrations (≤400 mg/L) had little inhibitory effect on the phosphorus recovery rate. However, when the concentration of SA was larger than 400 mg/L, the phosphorus recovery rate decreased significantly with increasing SA concentrations. The inhibition rate of 800 mg/L SA was about 3 times as large as that of 400 mg/L SA. It was worth noting that the inhibitory effect of SA on vivianite precipitation decreased with increasing initial pH and Fe/P molar ratios. Additionally, SA has no obvious influence on the composition of products, but the morphology of harvested crystals was transformed from branches to plates or rods in uneven sizes.

Introduction

As a necessary element for life activities of humans, animals and plants, phosphorus is barely renewable and has limited reserves. With the growth of global population and the improvement in living standards, the demand for phosphorus is on the increase. It was estimated that global reserve of phosphate rock can only be mined for 50 years (Hao et al., 2013), magnifying the problem of phosphorus shortages. In addition, about 1.3 million tons of phosphorus discharged into the wastewater treatment plants (WWTPs) every year (Li and Li, 2017), and finally was transferred into excess sludge after being treated (Huang et al., 2015; Park et al., 2017). If this part of phosphorus is recovered, it can meet 15%-20% of global phosphorus demand (Yuan et al., 2012). Therefore, the excess sludge is a suitable resource for phosphorus recovery, which can well alleviate global phosphorus shortages.

In terms of the phosphorus recovery methods, the struvite (magnesium ammonium phosphate, MAP) crystallization has attracted much attention (Ye et al., 2014; Wang et al., 2018a). But in fact, operating conditions of struvite crystallization are complex and its recovery efficiency is unsatisfactory (10%-50%) (Egle et al., 2015; Wilfert et al., 2018). In contrast, vivianite ($Fe_3(PO_4)_2{\cdot}8H_2O$) is characterized by natural ubiquity, high economic value and easy accessibility (Wu et al., 2019), thus being favored by the international academic circles. For example, vivianite has been detected in both septic tank sewage and sludge anaerobic systems (Azam and Finneran, 2014; Frossard et al., 1997; Seitz et al.,1973). Vivianite can be used as slow-release fertilizer and raw material for lithium iron phosphate ($LiFePO_4$). In addition, large high-purity vivianite crystals enjoy excellent collection value (Hao et al., 2018).

At present, a large number of studies have confirmed the feasibility of applying vivianite precipitation to the sludge anaerobic system to recover phosphorus (Cheng et al., 2015, 2017; Wilfert et al., 2016, 2018; Wang et al., 2019a). It has also

* Corresponding author.
E-mail: hudexiu@xaut.edu.cn (D. Hu).

https://doi.org/10.1016/j.jes.2020.04.007

been proved that it is a workable method to release phosphorus (P) and Fe from sludge phase into liquid phase through sludge pretreatment and then re-precipitation to get vivianite (Lin et al., 2017; Cao et al., 2019). For instance, Li et al. (2018) regulated the pH of supernatant rich in P and Fe after anaerobic fermentation to 8, and found that 99.1% of P in the supernatant formed vivianite. However, there are many organic compounds and metal ions in the sludge or sludge supernatant (Wang et al., 2016; Moragaspitiya et al., 2019), which will have effect on vivianite precipitation. It has been already found that humic acids, Al^{3+} and S^{2-} have adverse effects on the vivianite precipitation and the purity of harvested vivianite (Hao et al., 2018a; Lundager, 2019; Rothe et al., 2016). However, little attention has been paid to the impact of organic substances in excess sludge, especially the impact of a considerable amount (50%-90%) of extracellular polymeric substance (EPS) on vivianite crystallization (Urbain et al., 1993). Our research team has noted that EPS is generated in the anaerobic phosphorus release process of sludge (Hu et al., 2019). Moreover, it has been found that EPS specifically interacts with the surface of minerals, such as struvite (Huang et al., 2016; Wei et al., 2019; Hu, et al., 2018), hydroxyapatite (Malkaj et al., 2005), calcite (Manoli and Dalas, 2002), vaterite (Rao et al., 2016) and brushite (Ucar et al., 2015), and thus affecting the growth of these minerals. Therefore, it is of necessity to investigate the influence of EPS on vivianite precipitation.

The composition of EPS is extremely complex. Lin et al (2012, 2013) found that a substantial amount of EPS, which was excreted by the bacteria in the granular sludge, displayed properties similar to alginate. Therefore, sodium alginate (SA) was employed as EPS to identify its effect on vivianite crystallization in this study. The main objective of this study is to investigate the effect of SA on vivianite precipitation under different initial SA concentrations, pH values and Fe/P molar ratios. Additionally, the composition, morphology and settleability of harvested vivianite crystals were analyzed by X-ray diffraction (XRD), scanning electron microscope (SEM) and zeta potential, respectively. The results obtained in this study are expected to provide a theoretical foundation for phosphorus recovery by vivianite precipitation in the presence of EPS.

1. Materials and methods

1.1. Preparation of wastewater

Stock solutions were prepared to form artificial wastewater by dissolving an analytical reagent grade of $NaH_2PO_4{\cdot}2H_2O$ chemicals in distilled water to get an initial an initial PO_4^{3-} concentration of 10 mmol/L. 1.6 g/L SA solution was prepared and mixed with artificial wastewater before the experiments. Stock solution of 18 mmol/L $FeCl_2{\cdot}4H_2O$ was added to the solutions in the batch reactors immediately before the experiments were initiated, and the $FeCl_2$ solution was acidified to pH=5 in order to reduce Fe^{2+} oxidation.

1.2. Crystallization experiments

Batch experiments of vivianite precipitation were implemented in a serum bottle at 25 °C. The addition of $FeCl_2$ solution was carried out under N_2 continuously adding into the solution, and the initial pH was rapidly adjusted by 2 mol/L HCl and 2 mol/L NaOH solution. Next, the reaction was conducted at a stirring speed (500 r/min) for 60 min, as specified in Reaction (1). After the reaction, a mixed liquor sample of 50 mL was taken from reactors, and filtered by 0.45 μm cellulose acetate membrane for dissolved compound (PO_4^{3-} and Fe^{2+}) analysis. The precipitates were washed with distilled water and dried at 40 °C for crystal detection.

$$3Fe^{2+}+2PO_4^{3-}+8H_2O = Fe_3(PO_4)_2 \cdot 8H_2O \quad (1)$$

Under the reaction conditions of Fe/P=1.8 and pH=8.0, SA concentrations as 0, 100, 200, 400, 600 and 800 mg/L were set to explore the effect of SA concentration on vivianite precipitation. Moreover, the initial pH values 6.5, 7.0, 7.5, 8.0, 8.5 and 9.0 were built to investigate the effect of pH on vivianite precipitation. The initial Fe/P molar ratio was maintained at 1.8 in the presence of SA (800 mg/L) and absence of SA. Furthermore, the initial Fe/P molar ratios 1:1, 1.5:1, 1.8:1, 2.1:1 and 2.4:1 were chosen to evaluate the effect of Fe/P on vivianite precipitation in the presence of SA (800 mg/L) and absence of SA at an initial pH value of 8.0.

To examine the effect of SA on the settleability of vivianite crystals, 50 mL aqueous suspension was put in four 50-mL colorimetric tubes as soon as the experiments at different SA concentrations (0, 100, 400 and 800 mg/L) were accomplished. Then the colorimetric tubes were rapidly shaken at the same time and kept for sedimentation.

1.3. Calculation method

The phosphorus recovery rate (PRE, %) was calculated as follows:

$$PRE = \frac{(P_0 - P_t)}{P_0} \times 100\% \quad (2)$$

where, P_0 (mg/L) and P_t (mg/L) are the PO_4^{3-}-P concentrations before and after precipitation reaction, respectively.

The inhibition rate (IR, %) of SA on phosphorus recovery was defined as follows:

$$IR = \frac{(R_0 - R_i)}{R_0} \times 100\% \quad (3)$$

where, R_0 and R_i are the phosphorus recovery rate without and with SA respectively.

The supersaturation index (SI) of vivianite crystals was calculated by Eq. (4):

$$SI = \lg \frac{\left\{Fe^{2+}\right\}^3 \cdot \left\{PO_4^{3-}\right\}^2}{K_{SP}} \quad (4)$$

where, K_{SP} representes the solubility constant of vivianite at 25 °C, fixed at 10^{-36} (Al-Borno and Tomson, 1994; Nriagu, 1972) in this study; $\{Fe^{2+}\}$ and $\{PO_4^{3-}\}$ represent the ionic activity of Fe^{2+} and PO_4^{3-} respectively; SI was calculated by software PHREEQC (Parkhurst and Appelo, 1999).

1.4. Analysis method

PO_4^{3-}-P and Fe^{2+} were determined by ammonium molybdate spectrophotometric method and 10-phenanthroline spectrophotometric method (MEP, 2002). The zeta potential on the surface of vivianite crystals was measured by means of a potential instrument (Malvern / ZS, Malvern, England). The characteristics of recovered crystals were analyzed by a scanning electron microscope (VEGA3 XMU, TESCAN Brno, Czechia) and X-ray diffraction (Smart Lab, Rigaku, Japan).

2. Results and discussion

2.1. Effect of SA concentration on phosphorus recovery

The influence of SA concentration on vivianite precipitation at pH 8.0 and Fe/P ratio 1.8 is shown in Fig. 1. The SA at low

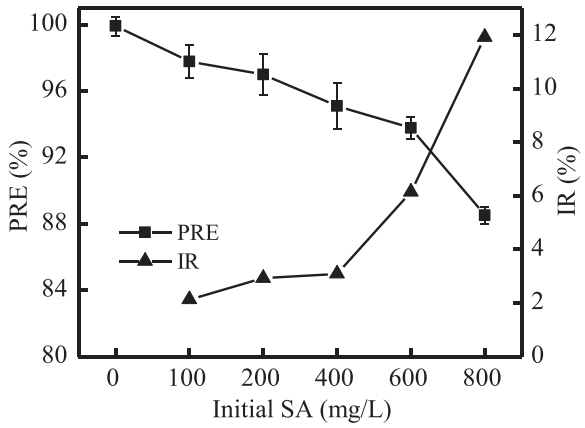

Fig. 1 – Effect of sodium alginate (SA) concentration on phosphorus recovery. pH=8.0, Fe/P=1.8, 25 °C,PRE: phosphorus recovery rate; IR: inhibition rate.

concentrations only exerted a relatively small effect on vivianite precipitation. The PRE value decreased from 99.91% to 95.09% as the concentration of SA ranged from 0 to 400 mg/L. When the concentration of SA increased to over 400 mg/L, the PRE value dropped considerably while the inhibition rate rose rapidly. To be specific, the PRE value decreased to 93.77% and 88.51% respectively at the SA concentration of 600 mg/L and 800 mg/L, while the IR value was 1.5 and 3 times respectively as large as that when the SA concentration was 400 mg/L. The results suggested that the high concentration of SA had an obvious inhibitory effect on phosphorus recovery by vivianite precipitation. The carboxyl groups (COOH) in SA could form a complex with divalent metal ions (Karthik and Meenakshi, 2015; Haug et al., 1967). Therefore, when SA was present in aqueous solution, on the one hand, carboxyl groups (COOH) could combine with Fe^{2+} to form a complex similar to gelatum (Liu et al., 2012), which consumed the amount of Fe^{2+} ready for the crystallization of vivianite; on the other hand, SA could adsorb and mask the growth activity points on the surface of vivianite crystals, which inhibited the growth of crystals (Wei et al., 2019).

2.2. *Effect of sa on phosphorus recovery at different pH values*

The PRE and IR as a function of pH (6.5–9.0) at Fe/P ratio of 1.8 in the absence and presence of SA (800 mg/L) are illustrated in Fig. 2a. In the absence of SA, PRE increased from 71.5% at initial pH of 6.5 to 96.8% at initial pH of 7.0, then increased slowly at initial pH of 7.0–8.0, and finally decreased slightly with further increase in initial pH. The observed PRE results were in agreement with previous works concerning vivianite precipitation of the fermentation supernatant of the sludge, where the optimum pH 8.0 was reported (Li et al., 2018; Li and Li, 2017). The PRE with and without the addition of 800 mg/L SA showed similar trend, but the PRE value with 800 mg/L SA was 2%-12% lower than that in the absence of SA.

To be specific, the IR value dropped sharply when pH was larger than 8.0. The IR value at pH 9.0 was 80% lower than that at pH 8.0. PO_4^{3-} concentration increased with the increase in pH due to the deprotonation of HPO_4^{2-}, $H_2PO_4^-$ and H_3PO_4 (Crutchik and Garrido, 2016, Lundager and Bruun, 2014), resulting in an increase in SI. As Fig. 2b depicted, SI of vivianite crystals increased from 10.22 to 15.68 with growing pH values, leading to a higher rate of crystallization. This was the reason for a decrease in inhibition rate with growing pH values. In addition, at a lower pH value, the phosphate protonation and hydrated Fe groups on the surface of vivianite crystals was high, which was conducive to the formation of a hydrogen bonding and surface complexation between vivianite crystals and SA (Wei et al., 2018), thereby intensifying its inhibitory effect due to its favorable adsorption.

2.3. *Effect of SA on phosphorus recovery at different Fe/P ratios*

Fig. 3a indicates the effect of initial Fe/P molar ratio on PRE at pH 8.0 in the presence and the absence of 800 mg/L SA. In either case, the PRE in the reaction solution increased first and then became stable with increasing Fe/P values. When Fe/P molar ratio exceeded 1.8, the PRE was basically unchanged, which was consistent with the optimal Fe/P range of 1.5–2.0 obtained by Wu et al. (2019). The PRE value in the presence of SA was always about 10% lower than that in the absence of SA. Meanwhile, the IR value decreased steadily with increasing Fe/P molar ratio, dropping from 16.0% to 6.8% when the Fe/P molar ration raised from 1:1 to 2.4:1. When Fe/P molar ratio was low, the complexation of SA with Fe^{2+} led to a strong inhibitory effect on vivianite precipitation; when Fe/P molar ratio was high, sufficient Fe^{2+} reacted with PO_4^{3-}, reducing the IR value. Besides, when the initial Fe/P molar ratio increased from 1:1 to 2.4:1, the SI of vivianite crystals also increased from 13.0 to 13.9 (Fig. 3b). There was a continuous fast growth at surface growth active sites at high supersaturation, while SA did not have enough time to be adsorbed onto these sites (Ilevbare, 2012). As a consequence, the inhibitory effect of SA on vivianite precipitation was weakened.

2.4. *Effect of SA on recovered crystals*

2.4.1. *Effect of SA on settleability of harvested crystals*

The settleability and zeta potential of harvested vivianite crystals at different concentrations of SA were exhibited in Fig. 4.

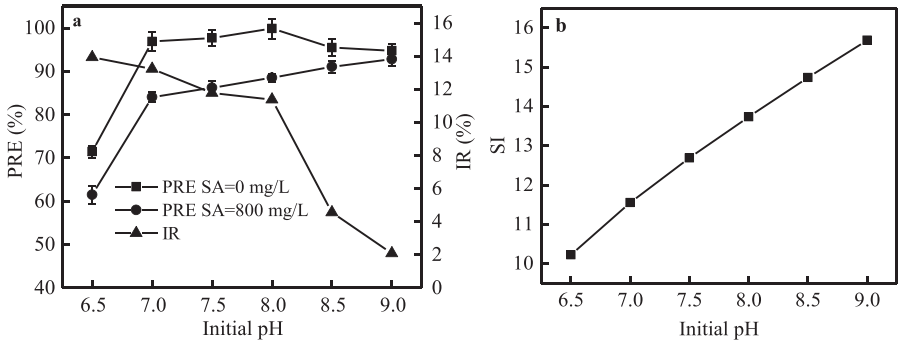

Fig. 2 – Effect of SA on phosphorus recovery at different pH values. Fe/P = 1.8, 25 °C, SI: supersaturation index.

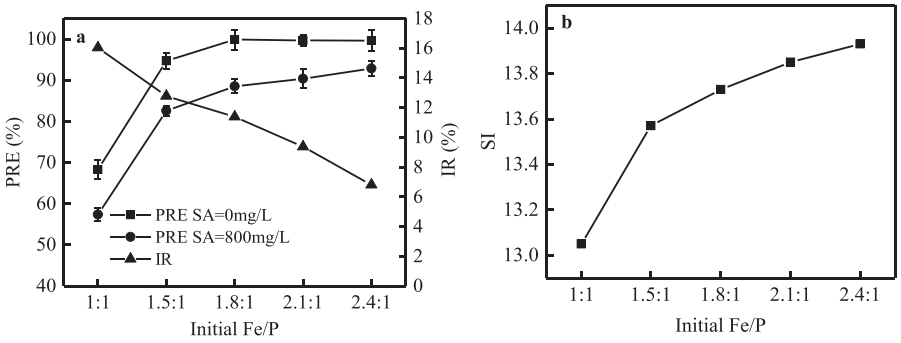

Fig. 3 – Effect of SA on vivianite precipitation at different Fe/P ratios. pH = 8.0, 25 °C.

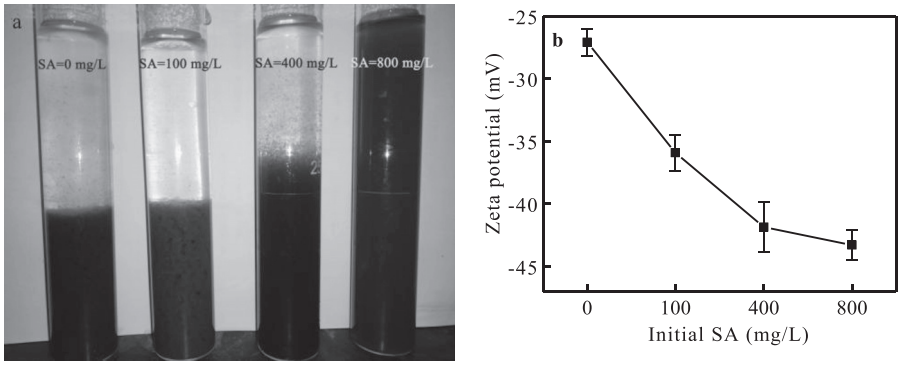

Fig. 4 – The suspension of vivianite crystal after 10 min sedimentation (a) and the variation of zeta potential of vivianite (b) under different SA concentrations. pH = 8.0, Fe/P = 1.8, 25 °C.

In the absence of SA, there appeared notable stratification after 10 min of settlement. As to the SA addition of 100 mg/L, obvious stratification was also observed and the supernatant was quite clear. This was because a small amount of SA and Fe^{2+} formed gelatum and played a role as flocculant, which was conducive to the formation of crystal settlement (Wu et al., 2019a). However, the settlement of recovered vivianite crystals was not enough and the zeta potential of the crystal surface decreased in the presence of 400 mg/L SA. When 800 mg/L SA was added into the reaction solution, the turbidity of the supernatant was extremely high after settling for 10 min and the zeta potential of the crystal surface decreased to -43.3 mV, which was 60% lower than that without SA. It was indicated by the results that the existence of high concentration SA reduced the settleability of vivianite crystals. This was possibly owing to the adsorption of SA on the surface of vivianite crystals, which decreased the zeta potential of the surface of vivianite crystals and enhanced the electrostatic repulsive force between vivianite crystals in solution (Wei et al., 2017). In addition, SA might adsorb and mask the growth points on the surface of the vivianite crystal to hinder the crystal growth, resulting in smaller crystal particles. According to the previous publication (Prot et al., 2019), when the vivianite crystallization method was applied to the phosphorus recovery in sludge, the smaller crystal tended to be bound to sludge flocs. Therefore, measures needed to be taken to realize the separation and recovery of crystal.

2.4.2. *Effect of SA on characteristics of vivianite crystals*

The XRD patterns of vivianite crystals at different SA concentrations at pH 8.0 and Fe/P 1.8 are shown in Fig. 5. No significant differences were seen on the position of peaks between the four harvested vivianite crystals. All the XRD patterns of the harvested vivianite crystals showed a series of

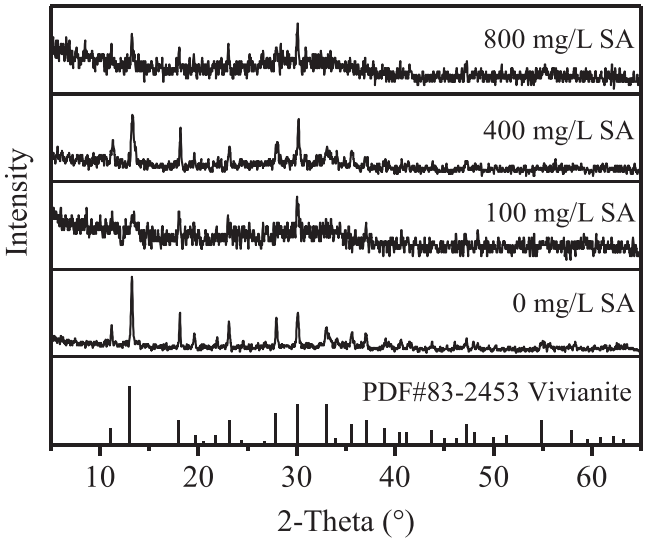

Fig. 5 – XRD spectra of recovered products at different SA concentrations.

diffraction peaks at 11.051°, 13.051°, 18.052°, 23.143°, 27.857°, 30.063° and 33.026° corresponding to Miller indices (110), (020), (200), (-201), (-131), (201) and (041) according to the analysis by software Jade 6.0. The result agrees with the standard spectra of vivianite crystals (PDF#83–2453). However, the presence of SA changed the relative intensity of crystal diffraction peaks. The lattice plane relative strength of vivianite crystals (110) and (020) decreased by degrees when the concentration of SA

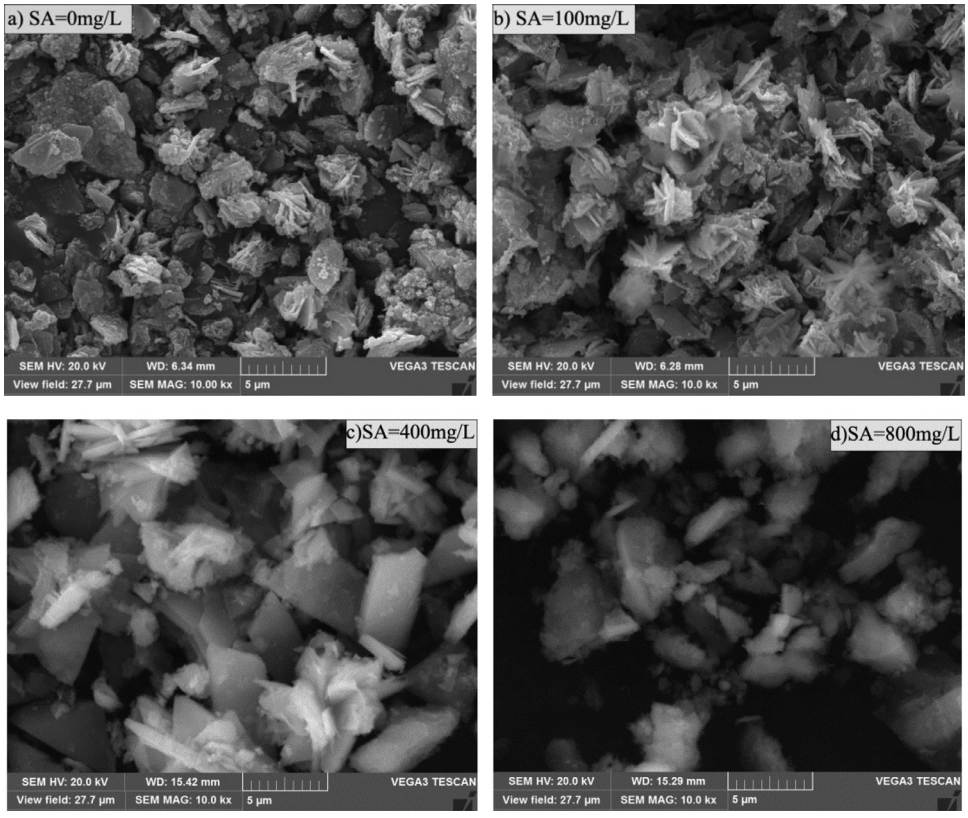

Fig. 6 – SEM images of recovered crystals at different SA concentrations.

increased gradually. It was implied that sodium alginate could change the morphology of vivianite crystals.

This phenomenon was further confirmed by SEM images of vivianite crystal at different SA concentrations (Fig. 6). Specifically, in the absence of SA, the shape of harvested crystals was branched, consistent with those reported in previous studies (Liu et al., 2018; Wang et al., 2018). The shape of the obtained vivianite crystals did not change at SA of 100 mg/L. When the concentration of SA increased to 400 mg/L, some vivianite crystals became smooth plates in shape. The vivianite crystals were rod-shaped or lump-shaped in uneven sizes in the absence of 800 mg/L. According to previous studies, the vivianite crystal morphology could be rod-shaped, strip-shaped, butterfly-shaped, branched and plate-shaped, which was closely related to reaction conditions (Tian et al., 2019; Wang et al., 2019; Zhou 2018; Lundager and Bruun, 2014). Speculatively, the reason for the change in vivianite crystal morphology could be that SA was adsorbed onto the surface of vivianite through static electricity, hydrogen bonding, chemical bonding and hydrophobicity (Dalase et al., 2007; Wei et al., 2019). Additionally, the change of vivianite crystal morphology would affect the utilization of vivianite, which is worth further study.

It was worth mentioning that the EPS content from activated sludge was in a range of 57–544 mg/g-MLVSS (Terna et al., 2019, Liu and Fang, 2002, Wilén et al., 2003, Adav and Lee, 2008, Pellicer-Nàcher et al., 2013). According to the simulation test of SA, EPS had a negative effect on the phosphorus recovery from sludge by vivianite crystallization. Nevertheless, the mitigation strategies of adjusting pH and supersaturation could help to improve vivianite crystallization and reduce the influence of EPS. For example, according to the study of Wei et al. (2017), constant composition technique might prevent the supersaturation of struvite from dropping during the crystallization process. Therefore, this method probably can be used to attenuate the inhibitory effect of EPS on the vivianite crystallization.

3. Conclusions

This study explored the effect of SA on vivianite precipitation under different conditions. The results showed that SA had an inhibitory effect on vivianite precipitation, which was weak at low SA concentration (<400 mg/L), but enhanced as the concentration increased. The inhibitory effect of SA on vivianite precipitation weakened with growing initial pH and Fe/P molar ratios. The morphology of harvested crystals changed from branches to plates and rods.

Acknowledgements

This work was supported by the State Key Laboratory of Eco-hydraulics in the Northwest Arid Region of China (No. 2016ZZKT-8).

REFERENCES

Adav, S.S., Lee, D.J., 2008. Extraction of extracellular polymeric substances from aerobic granule with compact interior structure. J. Hazard. Mater. 154, 1120–1126.

Azam, H.M., Finneran, K.T., 2014. Fe(III) reduction-mediated phosphate removal as vivianite ($Fe_3(PO_4)\cdot 8H_2O$) in septic system wastewater. Chemosphere 97, 1–9.

Al-Borno, A., Tomson, M.B., 1994. The temperature dependence of the solubility product constant of vivianite. Geochim. Cosmochim. Ac. 58, 5373–5378.

Cao, J.H., Wu, Y., Zhao, J.N., Jin, S., Aleem, M., Zhang, Q., et al., 2019. Phosphorus recovery as vivianite from waste activated sludge via optimizing iron source and pH value during anaerobic fermentation. Bioresour. Technol. 293, 122088.
Cheng, X., Chen, B., Cui, Y., Sun, D., Wang, X., 2015. Iron(III) reduction-induced phosphate precipitation during anaerobic digestion of waste activated sludge. Sep. Purif. Technol. 143, 6–11.
Cheng, X., Wang, J., Chen, B., Wang, Y., Liu, J.Q., Liu, L.B., 2017. Effectiveness of phosphate removal during anaerobic digestion of waste activated sludge by dosing iron(III). J. Environ. Manage. 193, 32–39.
Crutchik, D., Garrido, J.M., 2016. Kinetics of the reversible reaction of struvite crystallization. Chemosphere 154, 567–572.
Dalas, E., Barlos, K., Gatos, D., Manis, P., 2007. Effect of the cysteine-rich Mdm2 peptide in the crystal growth of hydroxyapatite in aqueous solution. Cryst. Growth Des. 7, 132–135.
Egle, L., Rechberger, H., Zessner, M., 2015. Overview and description of technologies for recovering phosphorus from municipal wastewater. Resour. Conserv. Recycl. 105, 325–346.
Frossard, E., Bauer, J.P., Lothe, F., 1997. Evidence of vivianite in $FeSO_4$-flocculated sludges. Water Res. 31 (10), 2449–2454.
Hao, X.D., Wang, C.C., van Loosdrecht, M.C.M., Hu, Y.S., 2013. Looking beyond struvite for P recovery. Environ. Sci. Technol. 47, 4965–4966.
Hao, X.D., Zhou, J., Wang, C.C., Mark, V.L., 2018. New product of phosphorus recovery-Vivianite. Acta Scientiae Circumstantiae 38 (11), 4223–4234.
Hao, X.D., Zhou, J., Wang, C.C., 2018a. Determination of interference factors of vivianite formation in anaerobic digestion of excess sludge. China Water Wastewater 34 (23), 1–7.
Haug, A., Myklestad, S., Larsen, B., Smidsrod, O., 1967. Correlation between chemical structure and physical properties of alginates. Acta Chem. Scand. 21, 768–778.
Hu, D.X., Zhang, Y., Zhu, L., Xiong, J.L., Li, L., 2019. Characteristics of phosphorus released and soluble microbial products in anaerobic conditions of sludge. China Environ. Sci. 38 (8), 2974–2980.
Hu, D.X., Zhang, Y., Luo, Y., 2018. Effect of organic matters on phosphorus recovery from wastewater by struvite crystallization method. China Water Wastewater 3, 1–6.
Huang, H., Liu, J., Wang, S., Jiang, Y., Xiao, D., Ding, L., et al., 2016. Nutrients removal from swine wastewater by struvite precipitation recycling technology with the use of $Mg_3(PO_4)_2$ as active component. Ecol. Eng. 92, 111–118.
Huang, W., Huang, W., Li, H., Lei, Z., Zhang, Z., Tay, J.H., et al., 2015. Species and distribution of inorganic and organic phosphorus in enhanced phosphorus removal aerobic granular sludge. Bioresour. Technol. 193, 549–552.
Ilevbare, G.A., Liu, H., Edgar, K.J., Taylor, L.S., 2012. Inhibition of solution crystal growth of ritonavir by cellulose polymers - factors influencing polymer effectiveness. Cryst. Eng. Comm. 14, 6503–6514.
Karthik, R., Meenakshi, S., 2015. Removal of Cr(VI) ions by adsorption onto sodium alginate-polyaniline nanofibers. Int. J. Biol. Macromol. 72, 711–717.
Li, R.H., Li, X.Y., 2017. Recovery of phosphorus and volatile fatty acids from wastewater and food waste with an iron-flocculation sequencing batch reactor and acidogenic cofermentation. Bioresour. Technol. 245 (Part A), 615–624.
Li, R.H., Wang, X.M., Li, X.Y., 2018. A membrane bioreactor with iron dosing and acidogenic co-fermentation for enhanced phosphorus removal and recovery in wastewater treatment. Water Res. 129, 402–412.
Lin, L., Li, R.H., Li, Y., Xu, J., Li, X.Y., 2017. Recovery of organic carbon and phosphorus from wastewater by Fe-enhanced primary sedimentation and sludge fermentation. Process Biochem. 54, 135–139.
Lin, Y.M., Bassin, J.P., van Loosdrecht, M.C., 2012. The contribution of exopolysaccharides induced struvites accumulation to ammonium adsorption in aerobic granular sludge. Water Res. 46, 986–992.
Lin, Y.M., Sharma, P.K., van Loosdrecht, M.C.M., 2013. The chemical and mechanical differences between alginate-like exopolysaccharides isolated from aerobic flocculent sludge and aerobic granular sludge. Water Res. 47 (1), 57–65.
Liu, H., Fang, H.H.P., 2002. Extraction of extracellular polymeric substances (EPS) of sludges. J. Biotechnol. 95, 249–256.
Liu, L., Wan, Y.Z., Xie, Y.D., Zhai, R., Zhang, B., Liu, J.D., 2012. The removal of dye from aqueous solution using alginate-halloysite nanotube beads. Chem. Eng. J. 187, 210–216.
Liu, J., Cheng, X., Qi, X., Li, N., Tian, J., Qiu, B., et al., 2018. Recovery of phosphate from aqueous solutions via vivianite precipitation: Thermodynamics and influence of pH. Chem. Eng. J. 349, 37–46.
Lundager Madsen, H.E., Bruun Hansen, H.C., 2014. Kinetics of crystal growth of vivianite, $Fe_3(PO_4)_2{\cdot}8H_2O$, from solution at 25, 35and 45 °C. J. Cryst. Growth 401, 82–86.
Lundager Madsen, H.E., 2019. Influence of calcium and aluminum on precipitation of vivianite, $Fe_3(PO_4)_2{\cdot}8H_2O$. J. Cryst. Growth 526, 125242.
Malkaj, P., Pierri, E., Dalas, E., 2005. The precipitation of Hydroxyapatite in the presence of sodium alginate. J. Mater. Sci. Mater. Med. 16, 733–737.
Manoli, F., Dalas, E., 2002. The effect of sodium alginate on the crystal growth of calcium carbonate. J. Mater. Sci. Mater. Med. 13, 155–158.
Ministry of Environment Protection, China (MEP), 2002. Standard Methods for the Examination of Water and Wastewater, 4th ed. Ministry of Environment Protection, Beijing, China.
Moragaspitiya, C., Rajapakse, J., Millar, G.J., 2019. Effect of Ca:Mg ratio and high ammoniacal nitrogen on characteristics of struvite precipitated from waste activated sludge digester effluent. J. Environ. Sci. 86 (12), 65–77.
Nriagu, J., 1972. Stability of vivianite and ion-pair formation in the system $Fe_3(PO_4)_2$-H_3PO_4-H_2O. Geoehim. Coemochim. Acta 36, 459–470.
Park, T., Ampunan, V., Maeng, S., Chung, E., 2017. Application of steel slag coated with sodium hydroxide to enhance precipitation-coagulation for phosphorus removal. Chemosphere 167, 91–97.
Parkhurst, D.L., Appelo, C.A.J., 1999. User's guide to PHREEQC (version 2): a computer program for speciation, batch-reaction, one-dimensional transport, and inverse geochemical calculations. Water-Resour. Invest. Rep. 99, 1–312.
Pellicer-Nàcher, C., Domingo-Félez, C., Mutlu, G.A., Smets, B.F., 2013. Critical assessment of extracellular polymeric substances extraction methods from mixed culture biomass. Water Res. 47, 5564–5574.
Prot, T., Nguyen, V.H., Wilfert, P., Dugulan, A.I., Goubitz, K., De Ridder, D.J., et al., 2019. Magnetic separation and characterization of vivianite from digested sewage sludge. Sep. Purif. Technol. 224, 564–579.
Rao, A., Vásquez-Quitral, P., Fernández, M.S., Berg, J.K., Sánchez, M., Drechsler, M., et al., 2016. pH-dependent schemes of calcium carbonate formation in the presence of alginates. Cryst. Growth Des. 16, 1349–1359.
Rothe, M., Kleeberg, A., Hupfer, M., 2016. The occurrence, identification and environmental relevance of vivianite in waterlogged soils and aquatic sediments. Earth-Sci. Rev. 158, 51–64.
Seitz, M.A., Riedner, R.J., Malhotra, S.K., Kipp, R.J., 1973. Iron-phosphate compound identification in sewage sludge residue. Environ. Sci. Technol. 7 (4), 354–357.
Terna lorhemen, O., Hamza, R.A., Zaghloul, M.S., Tay, J.H., 2019. Aerobic granular sludge membrane bioreactor (AGMBR): Extracellular polymeric substances (EPS) analysis. Water Res. 156, 305–314.
Tian, J.B., Cheng, X., Deng, S.Y., Liu, J.Q., Qiu, B., Dang, Y., et al., 2019. Inducing in situ precipitation of vivianite in a UCT-MBR system for enhanced removal and possible recovery of phosphorus from sewage. Environ. Sci. Technol. 53, 9045–9053.
Ucar, S., Bjørnøy, S.H., Bassett, D.C., Strand, B.L., Sikorski, P., Andreassen, J.P., 2015. Nucleation and growth of brushite in the presence of alginate. Cryst. Growth Des. 15, 5397–5405.
Urbain, V., Block, J.C., Manem, J., 1993. Bioflocculation in activated sludge: ananalytic approach. Water Res. 27 (5), 829–838.
Wang, C., Wang, S., Li, N., 2019. Phosphorus recovery through vivianite production by graphite enhanced microbial dissimilatory iron reduction. Acta Scientiae Circumstantiae 39 (10), 3325–3332.
Wang, F.X., Zheng, S.L., Qiu, H., Cao, C.Q., Tang, X., Hao, L.K., 2018. Ferrihydrite reduction and vivianite biomineralization mediated by iron reducing bacterium Shewanella oneidensis MR-4. Acta Microbiol. Sin. 58 (4), 573–583.
Wang, J., Ye, X., Zhang, Z., Ye, Z.L., Chen, S., 2018a. Selection of cost-effective magnesium sources for fluidized struvite crystallization. J. Environ. Sci. 70, 144–153.
Wang, R., Wilfert, P., Dugulan, I., Goubitz, K., Korving, L., Witkamp, G., et al., 2019a. Fe(III) reduction and vivianite formation in activated sludge. Sep. Purif. Technol. 220, 126–135.
Wang, Y.W., Xiao, Q.C., Zhong, H., Zheng, X., Wei, Y.S., 2016. Effect of organic matter on phosphorus recovery from sewage sludge subjected to microwave hybrid pretreatment. J. Environ. Sci. 39 (01), 29–36.
Wei, L., Hong, T., Liu, H., Chen, T., 2017. The effect of sodium alginate on struvite precipitation in aqueous solution: a kinetics study. J. Cryst. Growth 473, 60–65.
Wei, L., Hong, T., Li, X.Y., Li, M.Z., Zhang, Q., Chen, T.H., 2019. New insights into the adsorption behavior and mechanism of alginic acid onto struvite crystals. Chem. Eng. J. 358 pp. 1074–1072.
Wei, L., Hong, T., Hu, Z., Luo, L., Zhang, Q., Chen, T., 2018. Modeling surface acid-base properties of struvite crystals synthesized in aqueous solution. Colloids Surf. A Physicochem. Eng. Asp. 553, 237–243.
Wilfert, P., Dugulan, A.I., Goubitz, K., Korving, L., Witkamp, G.J., Van Loosdrecht, M.C.M., 2018. Vivianite as the main phosphate mineral in digested sewage sludge and its role for phosphate recovery. Water Res. 144, 312–321.
Wilfert, P., Mandalidis, A., Dugulan, A.I., Goubitz, K., Korving, L., Temmink, H., et al., 2016. Vivianite as an important iron phosphate precipitate in sewage treatment plants. Water Res. 104, 449–460.
Wilén, B.M.Jin, B., Lant, 2003. The influence of key chemical constituents in activated sludge on surface and flocculating properties. Water Res. 37, 2127–2139.
Wu, J., Zheng, H., Zhang, F., Zeng, R.J.X., Xing, B.S., 2019a. Iron-carbon composite from carbonization of iron-crosslinked sodium alginate for Cr(VI) removal. Chem. Eng. J. 362, 21–29.
Wu, Y., Luo, J., Zhang, Q., Aleem, M., Fang, F., Xue, Z., et al., 2019. Potentials and challenges of phosphorus recovery as vivianite from wastewater: a review. Chemosphere 226, 246–258.
Ye, Z.L., Shen, Y., Ye, X., Zhang, Z.J., Chen, S.H., Shi, J.W., 2014. Phosphorus recovery from wastewater by struvite crystallization: Property of aggregates. J. Environ. Sci. 26 (05), 991–1000.
Yuan, Z.G., Pratt, S., Batstone, D.J., 2012. Phosphorus recovery from wastewater through microbial processes. Curr. Opin. Biotechnol. 23 (6), 878–883.
Zhou, J., 2018. Recovery of phosphorus from anaerobic digested sludge-Preliminary study on formation mechanism of vivianite Ph.D. Thesis. Beijing University of Civil Engineering and Architecture.